frontiers | Frontiers in Materials

TYPE Original Research
PUBLISHED 10 May 2023
DOI 10.3389/fmats.2023.1192609



OPEN ACCESS

EDITED BY
Babatunde Okesola,
University of Nottingham,
United Kingdom

REVIEWED BY
Abshar Hasan,
University of Nottingham,
United Kingdom
Burak Derkus,
Ankara University, Türkiye

*CORRESPONDENCE
Weidong Huang,
weidong106@163.com
Wenchao Ji,
jiwc@ahstu.edu.cn

RECEIVED 23 March 2023
ACCEPTED 28 April 2023
PUBLISHED 10 May 2023

CITATION
Xiao X, Zheng Z, Yu H, Huang W and Ji W (2023), Microwave-assisted biosynthesis of nano silver and its synergistic antifungal activity against *Curvularia lunata* .
*Front. Mater.* 10:1192609.
doi: 10.3389/fmats.2023.1192609



# Microwave-assisted biosynthesis of nano silver and its synergistic antifungal activity against *Curvularia lunata*

Xiuhua Xiao[1], Zirui Zheng[2], Haibing Yu[2], Weidong Huang[2]* and Wenchao Ji[1]*

[1]College of Resources and Environment, Anhui Science and Technology University, Chuzhou, China, [2]College of Agriculture, Anhui Science and Technology University, Chuzhou, China

It is necessary to explore eco-friendly antimicrobial agents to resolve problems such as pathogen resistance and pesticide residues. In this study, *Mentha haplocalyx* leaf extract was applied to biosynthesize nano silver using a microwave-assisted method. The detailed properties of the nano silver were systematically revealed by several analytical methods. The antifungal activity of nano silver and synergistic antifungal effects of nano silver conjugated with pesticides against *Curvularia lunata* were determined. Pathogen invasion was significantly inhibited (57.3%) on detached and intravital maize leaves when the concentration of nano silver was 200 μg $mL^{-1}$, with an inhibition zone diameter of 12.5 ± 1.18 mm. In addition, a clear synergistic antifungal effect of nano silver conjugated with epoxiconazole was observed at volume ratios of 8:2 and 9:1, while the toxicity ratios were 1.18 and 1.11, respectively. These results not only provide a new avenue for pathogen management, but also enable reduced dosages of antibiotics and pesticides to mitigate or avoid emergence of drug-resistant pathogens.

KEYWORDS

**nano silver, antibacterial and antifungal, synergistic efficacy, biosythesis, microwave**

## 1 Introduction

Nanomaterials produced by nanotechnology exhibit unique properties, including the small-size effect and high surface area to volume ratio (Nasrollahzadeh et al., 2019; Kshtriya et al., 2021). Compared with their bulk counterparts, nanomaterials are versatile entities that have broad application potential in multiple fields (Jeevanandam et al., 2018; Khan and Saeed, 2019; Al-Shargabi et al., 2022). Physical, chemical, and biological methods for the synthesis of nanomaterials have been reported. In general, enormous energy and high pressure are necessary for physical synthesis (Barabadi et al., 2019; Zuorro et al., 2019), while toxic reductants and stabilizer are required for chemical synthesis (de Souza et al., 2019; Bahrulolum et al., 2021). Increasingly, therefore, researchers are turning their attention to biogenic synthesis to avoid these problems (Bulgarini et al., 2021; Saeki et al., 2021).

In view of emerging drug-resistant pathogens and pesticide residues that have been caused by long-term unreasonable use of chemicals, there is an urgent need for novel and efficient bacteriostatic agents. In recent years, bacteria, fungi, plant, and animal tissues have been used in the biosynthesis of multiple metallic and non-metallic nanomaterials (Huang et al., 2020; Dawadi et al., 2021; Zarei et al., 2021; Tian et al., 2022), in accordance with the

concept of green chemistry (Akter et al., 2020; Romano et al., 2022; Zaki et al., 2022). Among these nanomaterials, silver nanoparticles stand out because of their prominent antibacterial and antifungal activities compared with other nanomaterials like copper, zinc, magnesium, silicon, *etc. Terrabacter humi* was used to synthesize silver nanoparticles that exhibited strong antibacterial properties against *Escherichia coli* and *Pseudomonas aeruginosa* (Al-Otibi et al., 2023) Romano et al. reported that *Thermus thermophilus* could produce silver nanoparticles that effectively inhibited both Gram-positive and Gram-negative bacteria (Samad et al., 2021). Siver nanoparticles prepared using *Trichoderma harzianum* exhibited clear antifungal activity against *Fusarium fujikuroi*, *Rhizoctonia solani* and *Macrophomina phaselina* under greenhouse conditions (Alhomaidi et al., 2022). Not only microorganisms, but also plant tissues such as *Malva parviflora* (Jang et al., 2022), *Muki amaderaspatana* (Mohammed and Hawar, 2022), *Lawso niainermis* (Hwang et al., 2012), *Viola betonicifolia* (McShan et al., 2015) and *Moringa oleifera* (Li et al., 2018), have been used for biosynthesis of silver nanoparticles showing prominent antimicrobial effects.

Undoubtedly, antibiotics and pesticides contribute greatly to pathogen management, but the accompanying problem of pathogen resistance cannot be ignored. To re-duce their dosage, researchers began to conjugate antimicrobials with nanomaterials. Nano-Ags combined with three conventional antibiotics were tested against bacteria. Synergistic effects of nano-Ags and chloramphenicol were confirmed against *Enterococcus faecium* and *P. aeruginosa*. Synergistic activities of nano-Ags and ampicillin were found against *E. faecium*, *Streptococcus* mutans and *E. coli*. Synergistic effects of nano-Ags and kanamycin were verified against *Staphylococcus aureus*, *S. mutans*, *E. coli*, and *P. aeru-ginosa* (Hasson et al., 2019). Synergistic antibacterial activity of silver nanoparticles combined with three antibiotics against the multidrug resistant bacterium *Salmonella typhimurium* was evaluated by McShanet al. Dose-dependent inhibition was found with tetracycline and neomycin, while penicillin showed no synergistic activity (Huang et al., 2021). Li et al. combined silver nanoparticles with echinocandin and azole drugs. Combination of sub-lethal silver nanoparticles and echinocandin displayed prominent synergistic effects against *Candida albicans* (Abdul et al., 2022). Other antibiotics and pesticides, such as imipenem (Khalil et al., 2019), epoxiconazole (Huang et al., 2020), streptomycin sulfate (Pereira et al., 2012) and levofloxacin (Nuwamanya et al., 2022), have also been conjugated with silver nanoparticles to evaluate their synergistic activity against bacteria or fungi.

In this research, nano silver was biosynthesized using a microwave-assisted method mediated by *M. haplocalyx* leaf extract for the first time. Transmission electron microscopy (TEM), UV-vis spectrophotometry, scanning electron microscopy (SEM), atomic force microscopy (AFM), X-ray diffraction (XRD), energy dispersive X-ray analy-sis (EDX), Fourier transform infrared (FTIR) spectrometry, and zeta potentiometry were applied systematically for characterization. The sensitivity of *Curvularia lunata* to eight fungicides was determined using ahyphal growth rate method. Inhibition rate, agar diffusion, conidia germination, *in vivo* and *in vitro* inoculation were used to estimate the antifungal activity of the synthesized nano silver. In addition, synergistic antifungal effects of nano silver conjugated with five fungicides to which *C. lunata* was sensitive were tested using the toxicity ratio approach. The results not only provide a novel fungistat for inhibition of plant pathogens, but lay the foundations for development of nanopesticides to reduce the use of chemical pesticides.

# 2 Materials and methods

## 2.1 Pesticides and isolate

*M. haplocalyx* leaves, *C. lunata*, and $AgNO_3$ were preserved at the plant pathology laboratory, Anhui science and technology university. The concentration gradients of eight pesticides are provided in Table 1

## 2.2 Susceptibility of *C. lunata* to pesticides

Stock solutions (10 mg $mL^{-1}$) of eight pesticides were prepared in acetone and certain volumes were added to PDA (potato dextrose agar) plates at about 55 °C. A sterile hole puncher (φ = 8 mm) was used to obtain disks from PDA plates containing fungus grown for 7 days. One fungus disk was inoculated in the center of the pesticide-loaded PDA plate. Plates with sterile water were used as control. Treatment and control plates were incubated at 28 °C for 5–7 days.

## 2.3 Green synthesis and characterization of nano silver

### 2.3.1 Green synthesis of nano silver

M. haplocalyx dry leaf powder (~5 g) was added to a blue cap bottle containing de-ionized water (100 mL), which was then placed in a microwave at medium-high heat for 5 min. The leaf extract was then obtained by filtration through a Millipore filter (φ = 0.22 μm). For biosynthesis of nano silver, filtrate (10 mL) was mixed with deionized water and the concentration of $AgNO_3$ was set as 1 $mmol.L^{-1}$. The mixture was heated in a microwave for 2 min (Gao et al., 2017).

### 2.3.2 Characterization of nano silver

A UV-vis spectrophotometer (TU-1950, PERSEE, China) was used to establish the biosynthesis of nano silver. After heating for 2 min, 2 mL of solution was scanned over a wavelength range of 350–550 nm and the diluted filtrate was used as a blank. Sample was dripped on a copper grid until totally dried. TEM (JEM-2100F, JEOL, Japan) was utilized to determine the morphology and particle size of the biosynthesized nano silver. About 200 particles were selected randomly, and the size distribution was analyzed using ImageJ software. The sample was suspended in ethanol and added to substrate for SEM (S4800, Hitachi, Japan) analysis to determine the size of the nano silver agglomerates. The attached EDX system was used to verify the presence of elemental Ag. Nanoparticles on a mica surface were subjected to AFM (BioScope) in non-contact mode and the initial position of the nanoparticle was observed. FTIR was used to identify functional groups on the surface of the biogenic nano silver. Dried nano silver (~0.5 g) was mixed with KBr and pressed

**TABLE 1 Pesticides and their concentration gradients.**

| Fungicide | Concentration gradient (μg.mL$^{-1}$) | Manufacturer |
|---|---|---|
| epoxiconazole96% TC | 0.05, 0.2, 0.5, 2.0, 5.0 | Lier Chemical Co., LTD |
| difenoconazole 95% TC | 0.05, 0.2, 0.5, 2.0, 5.0 | Limin Chemical Co., LTD |
| Trifloxystrobin 98% TC | 0.2, 0.5, 2.0, 5.0,10.0 | Zhejiang Graminea Technology Co., LTD |
| metalaxyl 97% TC | 0.05, 0.2, 0.5, 2.0, 5.0 | Yifan Biotechnology Group Co., LTD |
| mancozeb 96% TC | 5.0, 10.0, 20.0, 50.0, 100.0 | Limin Chemical Co., LTD |
| Pyraclostrobin 95% TC | 0.2, 0.5, 2.0, 5.0,10.0 | Qingdao Hansheng Biotechnology Co., LTD |
| iprodione 96% TC | 0.05, 0.2, 0.5, 2.0, 5.0 | Jiangxi Heyi Chemical Co., LTD |
| thiophanate-methyl 95% TC | 5.0, 10.0, 20.0, 50.0, 100.0 | Jiangsu Yunfan Chemical Co., LTD |

**TABLE 2 Toxicity of fungicides against *C. lunata*.**

| Fungicides | $EC_{50}$ (μg.mL$^{-1}$) | 95% confidence interval (μg.mL$^{-1}$) | $R^2$ |
|---|---|---|---|
| epoxiconazole | 0.149 | 0.039-0.316 | 0.914 |
| difenoconazole | 0.419 | 0.171-0.916 | 0.978 |
| metalaxyl | 161.127 | — | 0.867 |
| trifloxystrobin | 2.939 | — | 0.951 |
| mancozeb | 110.289 | 41.086-1052234.763 | 0.964 |
| pyraclostrobin | 0.808 | 0.194-1.881 | 0.965 |
| iprodione | 0.435 | 0.105-1.385 | 0.888 |
| thiophanate-methyl | 309.636 | — | 0.928 |

/data not displayed.

into a thin pellet. A FTIR spectrum of nano silver was obtained in the range of 4,000–500 cm$^{-1}$. A zeta potentiometer was used to determine surface charge.

## 2.4 Antifungal effect of nano silver against *C. lunata*

### 2.4.1 Colony growth

Nano silver and PDA medium were mixed at a ratio of 1:9 (v/v) and the concentrations of nanoparticles were 10, 20, 50, 100, and 200 μg.mL−1. PDA medium with sterile water was the control. A fungus disk (φ = 8 mm) was inoculated in the center of the PDA plate and then incubated at 28 °C for 5–7 days. Each treatment or control was repeated 3 times. The inhibition rate was calculated using the following equation:

Inhibition rate (%) = *100%

### 2.4.2 Agar well diffusion

A spore suspension of C. lunata was prepared in sterile water and its concentration was adjusted to 106 mL−1 using a blood counting chamber. Subsequently, spore suspension (100 μL) was dripped and smeared evenly on solid PDA plates. Several wells were drilled with a hole puncher and samples (30 μL) of different concentrations (10, 20, 50, 100 and 200 μg.mL−1) of nano silver were dropped into the wells. The control well con-tained sterile water (30 μL). The inhibition zone diameter was measured after incubation at 28 °C for 2–3 days.

### 2.4.3 In vitro inoculation assay

Maize leaves (Anke985, AK985) were washed several times under running water and then dipped in 70% ethyl alcohol and 2% aqueous sodium hypochlorite solution for 1 min and 30 s, respectively. The sterilized leaves were then soaked in sterile water for 1 min to remove solution residue. Subsequently, the air-dried leaves were placed on solid PDA plates. A mixed solution (20 μL) containing different concentrations of nano silver and spore suspension was dripped onto the plates. Spore suspension (~20 μL) was added to the leaves as control. All plates were replicated 3 times and incubated at 25 °C for 72 h to observe infection in detached leaves under the microscope.

### 2.4.4 In vivo inoculation assay

Seeds of AK985 were sterilized by soaking in 5% aqueous sodium hypochlorite solution for 10 min and then rinsed three times with sterile water. The seeds were then placed in a germinating box with double sterilized gauze. Seven-day-old seedlings were transplanted into a pot containing 400 g of substrate and soil (3: 1, w/w). Plants were grown in a climate chamber with a cycle of 14 h

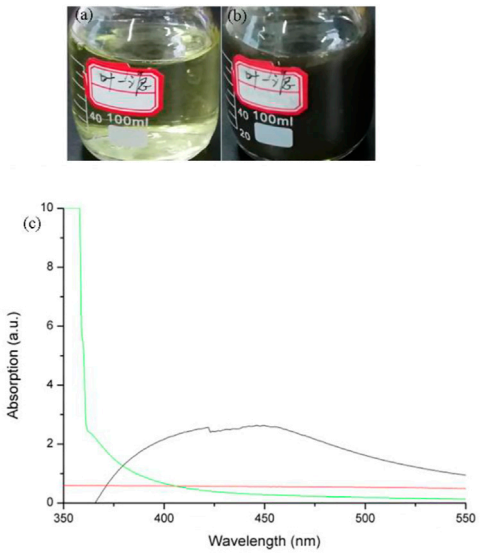


FIGURE1
Biosynthesis of nano silver using *M. haplocalyx* leaf extract. **(A)** Leaf extract without $AgNO_3$; **(B)** leaf extract with 1 mmol.$L^{-1}$ $AgNO_3$; **(C)** UV-vis spectra.

light at 25 ˚C and 10 h dark at 22 ˚C. Hoagland nutrient solution (Phygene Biotechnology Co. Ltd.) was applied once a week as fertilizer. After growing for 30 days, three treatments were sprayed onto the maize leaves as follows: 1) 5 mL/plant of sterile water, 2) 5 mL/plant of spore suspension (106 mL−1) containing 1% Tween-20, 3) 5 mL/plant of spore suspension (106 mL−1) containing 1% Tween-20 and 200 μg mL−1 nano silver. All treated plants were grown in the climate chamber described above, keeping the humidity above 80%. The infection on maize leaves was observed after incubation for 120 h.

## 2.5 Synergistic antifungal effect of nano silver and fungicides against *C. lunata*

The toxicities of the fungicides and nano silver were measured using ahyphal growth rate method. The EC50 (effective concentration at which fungal growth is inhibited by 50%) values were calculated using SPSS 16.0 software. According to the EC50 values, the most potent fungicides were selected for conjugation with nano silver using volume ratios of 0:10, 1:9, 2:8, 3:7, 4:6, 5:5, 6:4, 7:3, 8:2, 9:1, and 10:0. After thorough mixing, each conjugate was mixed with PDA medium at a ratio of 1:9 (v/v) at about 55 ˚C. The colony growth inhibition method was used to measure colony diameter. The synergistic activity of nano silver and fungicides was evaluated in terms of toxicity ratio (Huang et al., 2020). The synergistic activity assessment (toxicity ratio) of nano silver and epoxiconazole was determined by the following equations.

(1) Actual inhibition rate = $[(\varphi_{\text{control colony}} - \varphi_{\text{treatment colony}})/(\varphi_{\text{control colony}} - \varphi_{\text{fungusdisk}})]^{*}100\%$
(2) Theoretical inhibition rate= (Actual inhibition rate of A at medium concentration* percentage of A+ Actual inhibition rate of B at medium concentration* percentage of B) *100%;
(3) Toxicity ratio = Actual inhibition rate/Theoretical inhibition rate.

The combination activity shows synergistic when toxicity ratio was greater than 1; it shows antagonistic when toxicity ratio was less than 1; it shows additive when toxicity ratio was almost equal 1.

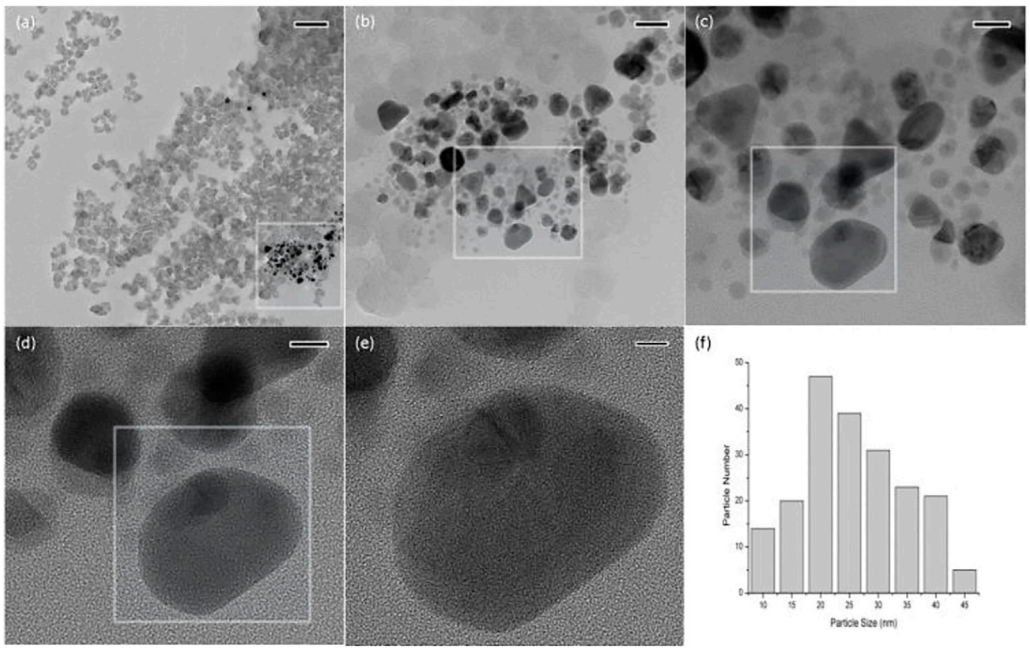


FIGURE 2
TEM images **(A–E)** and particle size distribution **(F)** of nano silver. The scale bar of **(A–E)** is 200, 50, 20, 10, and 5 nm, respectively.

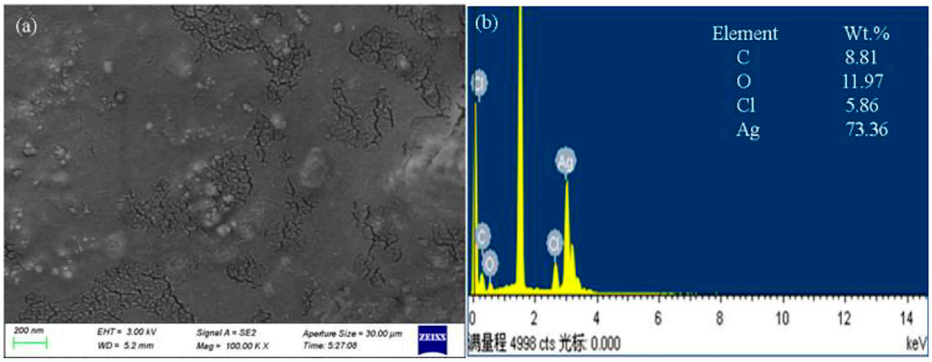


FIGURE 3
SEM image **(A)** and EDX spectrum **(B)** of nano silver.

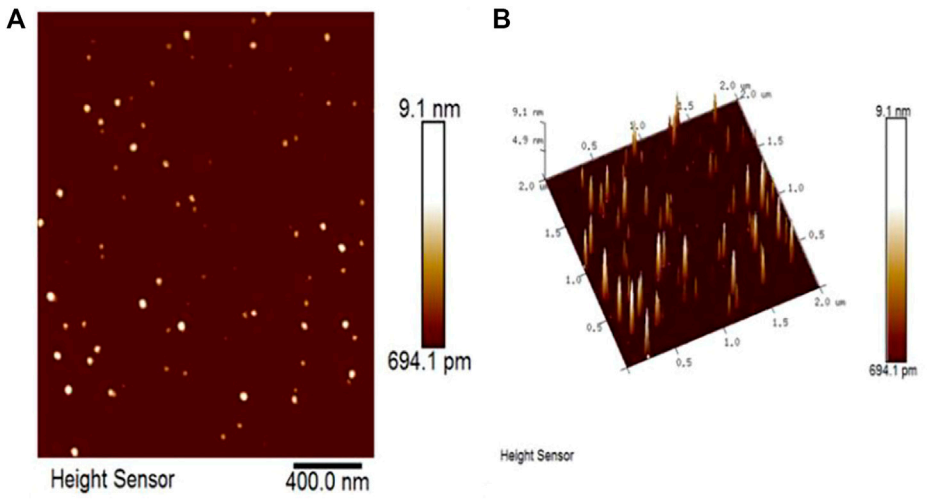


FIGURE 4
AFM image of nano silver. Morphological features **(A)** and 3D topographic image **(B)** of nano silver.

# 3 Results and discussion

## 3.1 Toxicity of fungicides against *C. lunata*

The potencies of the eight fungicides against *C. lunata* differed significantly (Table 2), with $EC_{50}$ values in the range of 0.149–309.636 μg $mL^{-1}$. The fungicides can be divided into those to which *C. lunata* is sensitive or insensitive according to the $EC_{50}$ value (Thangeswari et al., 2015; Gao et al., 2017). *C. lunata* was most sensitive to epoxiconazole, difenoconazole, trifloxystrobin, pyraclostrobin and iprodione, with epoxiconazole being the most effective of these fungicides. However, the antifungal activities of metalaxyl, mancozeb, and thiophanate-methyl against *C. lunata* were not outstanding, with thiophanate-methyl being the least effective. Maize Curvularia Leaf Spot is a global maize disease that causes severe reductions of yield and quality. Numerous fungicides with different antimicrobial mechanisms have been used to control this disease (Hassan et al., 2020; Sellami et al., 2021; Li et al., 2022). There is no doubt that chemical fungicides make a significant contribution to plant disease control, but the increasing prevalence of pathogen resistance requires urgent monitoring for drug resistance and screening for highly efficient fungicides with low risk of resistance. The fungicides identified through this process would provide a reference for management of Maize Curvularia Leaf Spot in the field.

## 3.2 Green synthesis of nano silver

The solution of *M. haplocalyx* leaf extract changed from faint yellow (Figure 1A) to black brown (Figure 1B) when it was heated with $AgNO_3$, indicating formation of nano silver (Huang et al., 2020; Al-Otibi et al., 2023). Green synthesis of nano silver mediated by plant extract is simple, eco-friendly, and cost-effective in contrast to

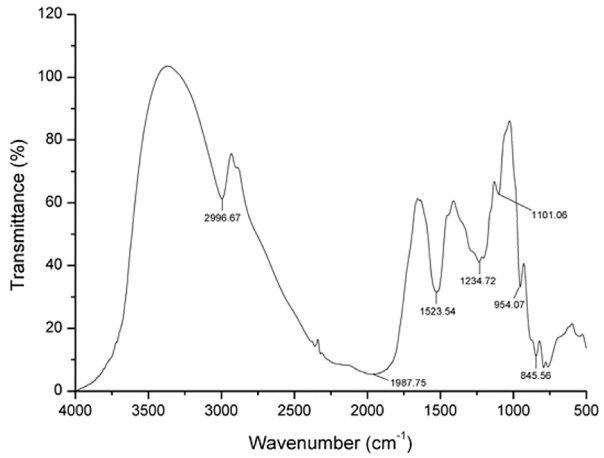


FIGURE 5
FTIR spectrum of biosynthesized nano silver.

traditional physical or chemical approaches. In addition, using microwave assistance requires less time compared with water bath heating. The UV-vis spectrum showed that there was strong absorbance at 420 nm, attributed to the characteristic absorption peak of nano silver (Khatami et al., 2017; Paul and Yadav, 2016). However, there were no obvious absorption peaks for leaf extract or $AgNO_3$ alone (Figure 1C). It is worth mentioning that the characteristic elemental absorption peak is not a definite value but a wavelength range, and particle size is positively correlated to the wavelength. It has been reported that when *Trachycar pusfortunei* was used to synthesize nano silver, the maximum absorption peak was at 462 nm, and the average particle size was about 88 nm (Khalil et al., 2019), which is much larger than that reported here.

## 3.3 Characterization of nano silver

### 3.3.1 TEM analysis

The morphology of nano silver is not exactly the same when synthesized using different living organisms or even the same one. As shown in Figure 2, most of the synthesized particles were near spherical, similar to previous reports (Khatami et al., 2017; Helmlinger et al., 2016; Mollahosseini et al., 2012). Some other shapes were also present, including triangular, rectangular and irregularly shaped. Helmlinger et al. reported that multiple morphologies of silver nanoparticles, including spheres, platelets, cubes, and rods, were prepared and their antibacterial activities were also measured (Hussain et al., 2019). Figure 2B shows that the sizes of synthesized particles were in the range of 6–48 nm and the average particle size was about 23 nm. The prominent antimicrobial activity of nanomaterials is closely related to their superfine size. It has been reported that the smaller the particle size, the stronger the antimicrobial activity (Hussain et al., 2019; Franzolin et al., 2022).

### 3.3.2 SEM and EDX analysis

The morphology of synthesized nano silver was also evaluated by SEM. The particles were almost spherical, either as individuals or gathered into clusters (Figure 3A). The elemental composition was determined using an EDX detector attached to the scanning electron microscope. Figure 3B shows a strong peak for elemental silver (Ag) at around 3 keV. The presence of other elements, including carbon C), oxygen O), chlorine (Cl) and unknown, might be due to components of plant extract. It has been reported that polyphenols and flavonoids present in plant extract are likely to reduce silver ion, and some inherent secondary metabolites, such as alkaloids and saponins, might contribute to the stability of nanoparticles (Binsalah et al., 2022).

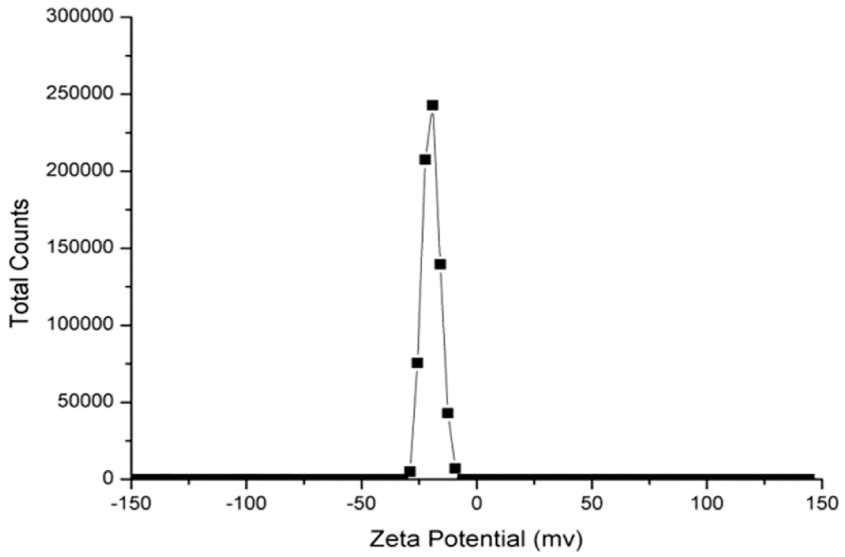


FIGURE 6
Zeta potential of green synthesized nano silver.

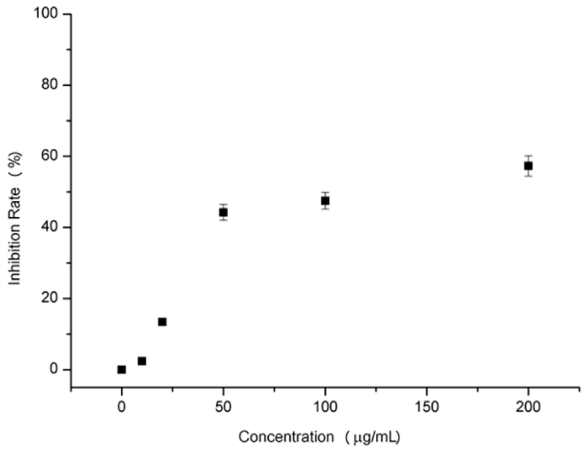


FIGURE 7
*C. lunata* colony growth inhibition by nano silver.

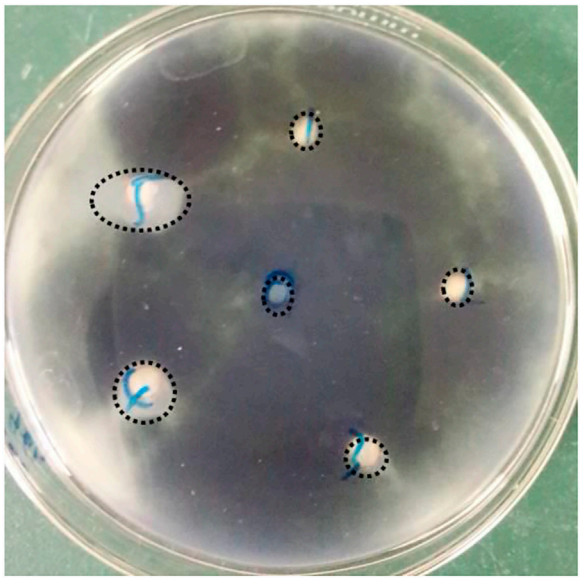

FIGURE 8
Inhibition zone caused by nano silver. Labels of 0, 1, 2, 3, 4, and 5 represent the concentration of nano silver was 0, 10, 20, 50, 100, and 200 μg $mL^{-1}$, respectively.

### 3.3.3 AFM analysis

The particular morphological features of the green synthesized nano silver were determined by AFM. The particles deposited on the substrate with uniform distribution (Figure 4A). The 3D topographic image is shown in Figure 4B.

### 3.3.4 FTIR analysis

The FTIR spectrum of synthesized nano silver was recorded, and the bioactive compounds that might be related to biosynthesis and stability of nano silver were investigated. The FTIR spectrum of biosynthesized nano silver contained bands at 2,996.67, 1987.75, 1523.54, 1234.72, 1101.06, 954.07, and 845.56 $cm^{-1}$ (Figure 5). The band observed at 2,996.67 $cm^{-1}$ indicates a C–H (alkane) group. The band at 1987.75 $cm^{-1}$ represents C=C (alkene) stretching. The peak seen at 1523.54 $cm^{-1}$ indicates a C–H (alkane) group. The bands at 1234.72 and 1101.06 $cm^{-1}$ are attributed to C–O (alcohol/ether) and C–N (amine) stretching, respectively. The bank appeared at 954.07 and 845.56 $cm^{-1}$ indicate a O-H and C-Cl group (Paul and Yadav, 2016; Toro et al., 2021; Al-Otibi et al., 2023; Khatami et al., 2017). These characteristic bands appearing on the surface of nano silver are due to the presence of proteins, flavonoids, phenolic compounds or other substances that contribute to capping and stabilization of nano silver (Liaqat et al., 2022).

### 3.3.5 Zeta potential analysis

To ascertain the surface charge of nano silver biosynthesized by *M. haplocalyx* leaf extract, the zeta potential was determined. Figure 6 shows that the zeta potential value was −19.7 mv, which indicates that the synthesized nano silver was relatively stable. Compared with physical and chemical approaches, plant- or microorganism-mediated synthesis of nano silver does not require extra capping or stability agents, since the presence of bioactive compounds prevents particle aggregation (Sathiyabama and Manikandan, 2018; Khodadadi et al., 2021).

## 3.4 Antifungal effect of nano silver

### 3.4.1 Inhibition rate

Amycelial growth rate method was used to determine the effects of nano silver at different concentrations against *C. lunata*. As shown in Figure 7, growth of *C. lunata* was inhibited in a concentration-dependent manner by nano silver. On the control plate, the colony covered the Petri dish (φ = 9 cm). The colony area decreased gradually as the concentration of nano silver was increased. At a concentration of 200 μg $mL^{-1}$, the colony diameter was 4.30 cm, and the inhibition rate reached 57.3%.

### 3.4.2 Inhibition zone diameter

An obvious inhibition zone will appear around the agar wells if there is antimicrobial activity. The zone diameter is positively correlated with inhibition (Figure 8). Table 3 shows that synthesized nano silver at high concentrations (≥50 μg $mL^{-1}$) exhibited antifungal activity against *C. lunata*. There appeared no inhibition zone at low concentrations (10 and 20 μg $mL^{-1}$), however, when the concentration increased to 200 μg $mL^{-1}$, the diameter reached 12.50 ± 1.18 mm. There is a positive relationship between nanoparticle diffusion in agar and inhibition zone diameter. Nano silver can diffuse more into agar well and obtain more chance to interact with *C. lunata* at a higher concentration, however the diffusion of lower concentration nano silver is limited. In addition to the agar well diffusion method, the filter paper diffusion approach has also been used to determine the inhibition zone diameter. The latter method is influenced by parameters such as volume of addition, type of nanoparticle and species of pathogen (Hasson et al., 2019; Huang et al., 2020; Al-Otibi et al., 2023).

**TABLE 3 Inhibition zone diameter of nano silver against *C. lunata*.**

| Concentrationofnano silver ($\mu g.mL^{-1}$) | Inhibition zone diameter (mm) |
|---|---|
| 0 | 0.00 ± 0.00 |
| 10 | 0.00 ± 0.00 |
| 20 | 0.00 ± 0.00 |
| 50 | 8.80 ± 0.96 |
| 100 | 9.15 ± 1.32 |
| 200 | 12.50 ± 1.18 |

### 3.4.3 *In vitro* inoculation

An *in vitro* inoculation assay was carried out to estimate the antifungal effect of nano silver against *C. lunata* on detached maize leaf (Huang et al., 2020). At the correct temperature, high humidity is essential for conidia germination and disease spot extension. For maize leaf inoculated with conidia suspension alone, there was obvious necrosis near the inoculation point and a large part of the leaf turned yellow as pathogen infection progressed (Figure 9A). However, maize leaf inoculated with conidia suspension and nano silver (200 $\mu g\ mL^{-1}$) suffered less pathogen damage and the leaf looked much healthier than the control (Figure 9B). The microscopic image of the control showed that most of the conidia germinated and the mycelia filled the whole leaf tissue (Figure 9C), while almost all of the conidia failed to germinate in the presence of nano silver and few mycelia appeared in the leaf tissue (Figure 9D). Conidia germination is the initial and indispensable step for pathogen invasion, so it is desirable to reduce the germination rate of conidia (Huang et al., 2020; Khleifat et al., 2022). Besides, the growth of germ tubes was significantly suppressed, and the integrity and permeability of cell membranes was also disrupted by silver nanoparticles (Jian et al., 2022). In the *in vitro* inoculation experiment, 200 $\mu g\ mL^{-1}$ nano silver synthesized by *M. haplocalyx* leaf extract prevented *C. Lunata* infection of detached maize leaves.

### 3.4.4 *In vivo* inoculation

An *in vivo* inoculation assay was conducted to evaluate the antifungal activity of nano silver against *C. lunata* on living maize leaf. Figure 10A shows that numerous sub-round lesions appeared on leaves inoculated with conidia suspension alone. However, leaves inoculated with a mixture of conidia suspension and 200 $\mu g\ mL^{-1}$ nano silver suffered few lesions (Figure 10B). Several factors, such as pathogen, environment, host plant and human activity, influence plant disease epidemics. The result confirmed that 200 $\mu g\ mL^{-1}$ nano silver could greatly reduce the incidence of disease. In the case of foliar inoculation, it can definitely inhibit extend of disease spots, but where did the nanparticles go or transport is an interesting task for further research (Pérez-de-Luque, 2017), and which will evaluate its safety to plants.

## 3.5 Synergistic antifungal effect of nano silver and epoxiconazole

On the basis of its $EC_{50}$ value, epoxiconazole was selected as the most potent antifungal to conjugate with nano silver for evaluation of synergistic antifungal activity. As shown in Table 4, the

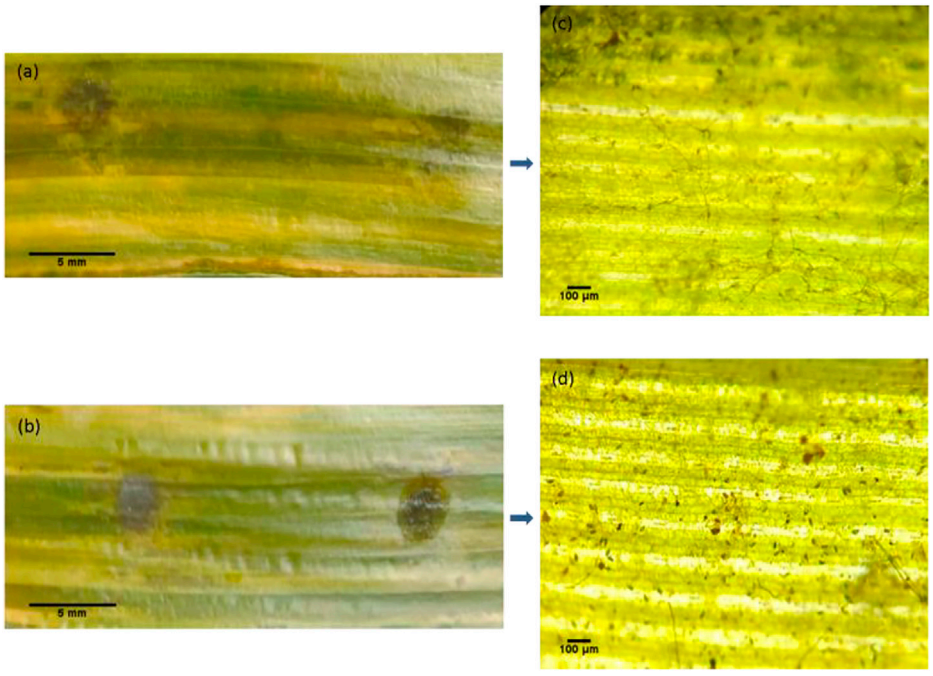


FIGURE 9
*In vitro* inoculation assay of nano silver against *C. lunata*. **(A)** Detached maize leaf inoculated with conidia suspension; **(B)** detached maize leaf inoculated with conidia suspension and 200 $\mu g\ mL^{-1}$ nano silver; **(C)** and **(D)** show microscopic images of the local regions of **(A)** and **(B)**.


FIGURE 10
*In vivo* inoculation assay of nano silver against *C. lunata*. **(A)** Maize leaf inoculated with conidia suspension; **(B)** maize leaf inoculated with conidia suspension and 200 μg $mL^{-1}$nano silver.

**TABLE 4 Toxicity ratios of nano silver and epoxiconazole against *C. lunata*.**

| Volume ratio | Actual inhibition rate (%) | Theoretical inhibition rate (%) | Toxicity ratio |
|---|---|---|---|
| 0:10 | 57.78 | 57.78 | 1.00 |
| 1:9 | 48.61 | 49.55 | 0.98 |
| 2:8 | 49.63 | 51.13 | 0.97 |
| 3:7 | 50.35 | 53.26 | 0.95 |
| 4:6 | 52.65 | 52.89 | 1.00 |
| 5:5 | 51.66 | 50.56 | 1.02 |
| 6:4 | 52.31 | 51.74 | 1.01 |
| 7:3 | 54.98 | 52.39 | 1.05 |
| 8:2 | 64.32 | 54.63 | 1.18 |
| 9:1 | 63.33 | 56.87 | 1.11 |
| 10:0 | 52.85 | 52.85 | 1.00 |

conjugation effect was divided into two parts: additive and synergistic. In particular, there was obvious synergy at volume ratios of 8:2 and 9:1 for nano silver and epoxiconazole, and the toxicity ratios were 1.18 and 1.11, respectively. At other volume ratios the effect was additive. The result demonstrated that biosynthesized nano silver could produce a synergistic antifungal effect at specific composition ratios, similar to a previous report (Huang et al., 2020). It has been reported that there was an antagonistic effect against *Valsa mali* when green synthesized nano silver using Trachycarpus fortune was conjugated with iprodione (Khalil et al., 2019), but there was no antagonistic effect in this experiment. Nano silver has also been conjugated with other antibiotics to determine their antibacterial effect, including imipenem (Hasson et al., 2019) and ampicillin (Khleifat et al., 2022).

## 4 Conclusion

In this experiment, *M. haplocalyx* leaf extract was successfully used with microwave assistance to rapidly synthesize nano silver. The nanoparticles were most near spherical, and the average diameter was about 23 nm. *In vivo* and *in vitro* assays demonstrated that nano silver (200 μg $mL^{-1}$)

not only effectively inhibited colony growth of C. lunata but also restricted conidia germination and disease spot expansion on detached and live maize leaves. In addition, toxicity and resistance of eight fungicides against *C. lunata* were evaluated using a mycelial growth rate method. The fungicides to which *C. lunata* was sensitive or insensitive were identified. The results are of great significance for plant disease management. In order to achieve the goal of reducing chemical pesticides and increasing efficiency, biosynthesized nano silver was conjugated with epoxiconazole (the most effective fungicide). There was obvious synergistic antifungal activity when the volume ratio of nano silver and fungicide was 8:2 and 9:1, and no antagonistic effect was observed. Such results not only provide a novel fungistat to control plant disease, but also lay the foundations for development of nano pesticides.

## Data availability statement

The original contributions presented in the study are included in the article/Supplementary Material, further inquiries can be directed to the corresponding author.

## Author contributions

XX and ZZ carried out the experiments and measurements and drafted the manuscript. HY participated in the discussion. WH and WJ contributed to the design of the experiment and analysis of the results in this paper. All authors read and approved the final manuscript.

## Funding

The Natural Science Foundation of Anhui Province (2108085QB56).

## Acknowledgments

This work was funded by the Key Research and Development Program of Anhui Prov-ince(202004a06020004, 202104a06020001), The Natural Science Foundation of Anhui Province (2108085QB56), Talent Projects of Anhui Science and Technology University (No. ZHYJ201802), and the Innovation project of university students (S202110879231). We thank International Science Editing (http://www.internationalscienceediting.com) for editing this manuscript.

## Conflict of interest

The authors declare that the research was conducted in the absence of any commercial or financial relationships that could be construed as a potential conflict of interest.

## Publisher's note

All claims expressed in this article are solely those of the authors and do not necessarily represent those of their affiliated organizations, or those of the publisher, the editors and the reviewers. Any product that may be evaluated in this article, or claim that may be made by its manufacturer, is not guaranteed or endorsed by the publisher.

## References

Abdul, S., Kadhem, S., and Salman, K. (2022). Antimicrobial effect of silver nanoparticles with *Kluyvera cryocrescens* and biofilm cultures. *LifeSci. Arch.* 7, 2130–2138.

Al-Otibi, F., Yasin, M. T., Al-Askar, A. A., and Maniah, K. (2023). Green biofabrication of silver nanoparticles of potential synergistic activity with antibacterial and antifungal agents against some nosocomial pathogens. *Microorganisms* 11, 945–965. doi:10.3390/microorganisms11040945

Al-Shargabi, M., Davoodi, S., Wood, D. A., Al-Musai, A., Rukavishnikov, V. S., and Minaev, K. M. (2022). Nanoparticle applications as beneficial oil and gas drilling fluid additives: A review. *J. Mol. Liq.* 352, 118725–118760. doi:10.1016/j.molliq.2022.118725

Alhomaidi, E., Jasim, S. A., Amin, H. I., Nobre, M. A. L., Khatami, M., Jalil, A. T., et al. (2022). Biosynthesis of silver nanoparticles using *Lawsonia inermis* and their biomedical application. *IET Nanobiotechnol* 16, 284–294. doi:10.1049/nbt2.12096

Bahrulolum, H., Nooraei, S., Javanshir, N., Tarrahimofrad, H., Mirbagheri, V. S., Easton, A. J., et al. (2021). Green synthesis of metal nanoparticles using microorganisms and their application in the agri food sector. *J. Nanobiotechnol.* 19, 86–111. doi:10.1186/s12951-021-00834-3

Barabadi, H., Mahjoub, M. A., Tajani, B., Ahmadi, A., Junejo, Y., and Saravanan, M. (2019). Emerging theranostic biogenic silver nanomaterials for breast cancer: A systematic review. *J. Clust. Sci.* 30, 259–279. doi:10.1007/s10876-018-01491-7

Binsalah, M., Devanesan, S., Alsalhi, M. S., Nooh, A., Alghamdi, O., and Nooh, N. (2022). Biomimetic synthesis of silver nanoparticles using Ethyl acetate extract of Urtica diocia leaves, characterizations and emerging antimicrobial activity. *Microorganisms* 10, 789–802. doi:10.3390/microorganisms10040789

Bulgarini, A., Lampis, S., Turner, R. J., and Vallini, G. (2021). Biomolecular composition of capping layer and stability of biogenic selenium nanoparticles synthesized by five bacterial species. *Microb. Biotechnol.* 14, 198–212. doi:10.1111/1751-7915.13666

Dawadi, S., Katuwal, S., Gupta, A., Lamichhane, U., Thapa, R., Jaisi, S., et al. (2021). Current research on silver nanoparticles: Synthesis, characterization, and applications. *J. Nanomater.* 2021, 1–23. doi:10.1155/2021/6687290

de Souza, C. D., Nogueira, B. R., and Rostelato, M. (2019). Review of the methodologies used in the synthesis gold nanoparticles by chemical reduction. *J. Alloys Compd.* 798, 714–740. doi:10.1016/j.jallcom.2019.05.153

Franzolin, M. R., Courrol, D. D. S., Barreto, S. D. S., and Courrol, L. C. (2022). *Eugenia uniflora* L. silver and gold nanoparticle synthesis, characterization, and evaluation of the photoreduction process in antimicrobial activities. *Microorganisms* 10, 999–1011. doi:10.3390/microorganisms10050999

Gao, S. G., Ni, X., Li, Y. Y., Fu, K. H., Yu, C. J., Gao, J. X., et al. (2017). Sod gene of *Curvularia lunata* is associated with the virulence in maize leaf. *J. Integr. Agr.* 16, 874–883. doi:10.1016/s2095-3119(16)61513-7

Hassan, M. A. U., Butt, I., Khan, I. H., Javaid, A., and Shad, N. (2020). Comparative efficacy of three fungicides for *in vitro* control of *Curvularia lunata*. *Mycopath* 18, 47–52.

Hasson, S. O., Al-Awady, M. J., Al-Hamadani, A. H., and Al-Azawi, I. H. (2019). Boosting antimicrobial activity of imipenem in combination with silver nanoparticles towards *S. fonticola* and Pantoeasp. *Nano Biomed. Eng.* 11, 200–214. doi:10.5101/nbe.v11i2.p200-214

Helmlinger, J., Sengstock, C., Grob-Heitfeld, C., Mayer, C., Schildhauer, T. A., Koller, M., et al. (2016). Silver nanoparticles with different size and shape: Equal cytotoxicity, but different antibacterial effects. *RSC Adv.* 6, 18490–18501. doi:10.1039/c5ra27836h

Huang, W. D., Wang, J., Wang, Z. X., and Yu, H. B. (2021). Synergistic antimicrobial activity of silver nanoparticles combined with streptomycin sulfate against gram-negative and gram-positive bacteria. *Mol. Cryst. Liq. Cryst.* 714, 80–88. doi:10.1080/15421406.2020.1856610

Huang, W. D., Yan, M. H., Duan, H. M., Bi, Y. L., Cheng, X. X., and Yu, H. B. (2020). Synergistic antifungal activity of green synthesized silver nanoparticles and

epoxiconazole against *Setosphaeria turcica*. *Setosphaeria Turc. J. Nanomater.* 3, 1–7. doi:10.1155/2020/9535432

Hussain, A., Alajmi, M. F., Khan, M. A., Pervez, S. A., Ahmed, F., Amir, S., et al. (2019). Biosynthesized silver nanoparticles (AgNP) from *Pandanus odorifer* leaf extrsct exhibits anti-metastasis and anti-biofilm potentials. *Front. Microbiol.* 10, 8–26. doi:10.3389/fmicb.2019.00008

Hwang, I. S., Hwang, J. H., Choi, H., Kim, K. J., and Lee, D. G. (2012). Synergistic effects between silver nanoparticles and antibiotics and the mechanisms involved. *J. Med. Microbiol.* 61, 1719–1726. doi:10.1099/jmm.0.047100-0

Jang, Y. P., Zhang, X. Y., Zhu, R. X., Li, S. L., Sun, S. Y., Li, W. Q., et al. (2022). *Viola betonicifolia*-mediated biosynthesis of silver nanoparticles for improved biomedical applications. *Front. Microbiol.* 13, 891144. doi:10.3389/fmicb.2022.891144

Jeevanandam, J., Barhoum, A., Chan, Y. S., Dufresne, A., and Danquah, M. K. (2018). Review on nanoparticles and nanostructured materials: History, sources, toxicity and regulations. *Beilstein J. Nanotechnol.* 9, 1050–1074. doi:10.3762/bjnano.9.98

Jian, Y. Q., Chen, X., Ahmed, T., Shang, Q. H., Zhang, S. A., Ma, Z. H., et al. (2022). Toxicity and action mechanisms of silver nanoparticles against the mycotoxin-producing fungus *Fusarium graminearum*. *J. Adv. Res.* 38, 1–12. doi:10.1016/j.jare.2021.09.006

Khan, I., and Saeed, K. (2019). Nanoparticles: Properties, applications and toxicities *Arab. J. Chem.* 12, 908–931. doi:10.1016/j.arabjc.2017.05.011

Khleifat, K., Qaralleh, H., Al-Limoun, M., Alqaraleh, M., Hajleh, M. N., Al-Frouhk, R., et al. (2022). Antibacterial activity of silver nanoparticles synthesized by *Aspergillus flavus* and its synergistic effect with antibiotics. *J. Pure Appl. Microbiol.* 16, 1722–1735. doi:10.22207/jpam.16.3.13

Khodadadi, S., Mahdinezhad, N., Fazeli-Nasab, B., Heidari, M. J., Fakheri, B., and Miri, A. (2021). Investigating the possibility of green synthesis of silver nanoparticles using *Vaccinium arctostaphlyos* extract and evaluating its antibacterial properties. *Biomed. Res. Int.* 2021, 1–13. doi:10.1155/2021/5572252

Kshtriya, V., Koshti, B., and Gour, N. (2021). Green synthesized nanoparticles: Classification, synthesis, characterization, and applications. *Compr. Anal. Chem.* 94, 173–222.

Li, H., Wang, L. H., Chai, Y. F., Cao, Y. B., and Lu, F. (2018). Synergistic effect between silver nanoparticles and antifungal agents on *Candida albicans* revealed by dynamic surface-enhanced Raman spectroscopy. *Nanotoxicology* 10, 1230–1240. doi:10.1080/17435390.2018.1540729

Li, T., Huang, W. D., and Yu, H. B. (2022). Synergistic antimicrobial effect of silver nanoparticles conjugated with iprodione against *Valsa mali*. *Materials* 15, 5147–5156. doi:10.3390/ma15155147

Liaqat, N., Jahan, N., Rahman, K., Anwar, T., and Qureshi, H. (2022). Green synthesized silver nanoparticles: Optimization, characterization, antimicrobial activity, and cytotoxicity study by hemolysis assay. *Front. Chem.* 10, 952006. doi:10.3389/fchem.2022.952006

McShan, D., Zhang, Y., Deng, H., Ray, P. C., and Yu, H. T. (2015). Synergistic antibacterial effect of silver nanoparticles combined with ineffective antibiotics on drug resistant *Salmonella typhimurium* DT104. *J. Environ. Sci. Health C.* 33, 369–384. doi:10.1080/10590501.2015.1055165

Mohammed, G. M., and Hawar, S. N. (2022). Green biosynthesis of silver nanoparticles from Moringaoleifera leaves and its antimicrobial and cytotoxicity activities. *Inter. J. Biomater.* 1, 1–10. doi:10.1155/2022/4136641

Mollahosseini, A., Rahimpour, A., Jahamshahi, M., Peyravi, M., and Khavarpour, M. (2012). The effect of silver nanoparticle size on performance and antibacteriality of polysulfone ultrafiltration membrane. *Desalination* 306, 41–50. doi:10.1016/j.desal.2012.08.035

Nasrollahzadeh, M., Sajadi, S. M., Sajjadi, M., and Issaabadi, Z. (2019). An introduction to nanotechnology. *Interface Sci. Technol.* 28, 1–27.

Nuwamanya, A. M., Runo, S., and Mwangi, M. (2022). *In-vitro* sensitivity of *Alternaria solani* isolates to azoxystrobin and difenoconazole fungicides in Kenya and detection of *Cyt* b mutations associated with azoxystrobin resistance. *Crop Prot.* 158, 106010. doi:10.1016/j.cropro.2022.106010

Paul, N. S., and Yadav, R. P. (2016). A simple biogenic method for the synthesis of silver nanoparticles using *Syngonium podophyllum*, an ornamental plant. *MJM J. Med. Sci.* 3, 111–115. doi:10.5005/jp-journals-10036-1103

Pereira, A. V. S., Martins, R. B., Michereff, S. J., Silva, M. B., and Câmara, M. P. S. (2012). Sensitive of *Lasiodiplodia thebromae* from Brazilian papaya orchards to MBC and DMI fungicides. *Eur. J. Plant Pathol.* 132, 489–498. doi:10.1007/s10658-011-9891-2

Pérez-de-Luque, A. (2017). Interaction of nanomaterials with plants: What do we need for real applications in agriculture? *Front. Env. Sci.* 5, 12–18. doi:10.3389/fenvs.2017.00012

Romano, I., Vitiello, G., Gallucci, N., Girolamo, R. D., Cattaneo, A., Poli, A., et al. (2022). Extremophilic microorganisms for the green synthesis of antibacterial nanoparticles. *Microorganisms* 10, 1885–1904. doi:10.3390/microorganisms10101885

Saeki, E. K., Yamada, A. Y., de Araujo, L. A., Anversa, L., Garcia, D. O., Souza, R. L. B., et al. (2021). Subinhibitory concentrations of biogenic silver nanoparticles affect motility and biofilm formation in *Pseudomonas aeruginosa*. Front. Cell. Infect. Microbiol. 11, 656984. doi:10.3389/fcimb.2021.656984

Samad, N., Farooq, S., Khaliq, S., Khan, S. A. M., Alam, M., Mustafa, S., et al. (2021). Biosynthesis of silver nanoparticles from *Mukia maderaspatana* and their biological activities. *Pak. J. Pharm. Sci.* 34, 1837–1847.

Sathiyabama, M., and Manikandan, A. (2018). Application of copper-chitosan nanoparticles stimulate growth and induce resistance in finger millet (*Eleusine coracana* Gaertn.) plants against blast disease *J. Agric. Food. Chem.* 66, 1784–1790. doi:10.1021/acs.jafc.7b05921

Sellami, H., Khan, S. A., Ahmad, I., Alarfaj, A. A., Hirad, A. H., and Al-Sabri, A. E. (2021). Green synthesis of silver nanoparticles using *Olea europaea* leaf extract for their enhanced antibacterial, antioxidant, cytotoxic and biocompatibility applications. *Int. J. Mol. Sci.* 22, 12562–12577. doi:10.3390/ijms222212562

Thangeswari, S., Sornakili, A., Manoranjitham, S. K., and Tha, V. (2015). *In vitro* screening of fungicides and antagonists against leaf blight of gloriosa superb incited by *Curvularia lunata*. *Ann. Plant Soil Res.* 17, 347–350.

Tian, S., Hu, Y., Chen, X., Liu, C., Xue, Y., and Han, B. (2022). Green synthesis of silver nanoparticles using sodium alginate and tannic acid: Characaterization and anti-*S. aureus* activity. *Int. J. Biol. Macromol.* 195, 515–522. doi:10.1016/j.ijbiomac.2021.12.031

Toro, L. D., Rodríguez-Félix, F., Moreno-Vásquez, M. J., Tapia-Hernández, J. A., Quintero-Reyes, I. E., Lopez-Cota, A. G., et al. (2021). Sustainable-green synthesis of silver nanoparticles using safflower (Carthamus tinctorius L.) waste extract and its antibacterial activity *Heliyon* 7, 1–11.

Zaki, S. A., Ouf, S. A., Abd-Elsalam, K. A., Asrn, A. A., Hassan, M. M., Kalia, A., et al. (2022). Trichogenic silver-based nanoparticles for suppression of fungi involved in damping-off of cotton seedlings. *Microorganisms* 10, 344–351. doi:10.3390/microorganisms10020344

Zarei, M., Karimi, E., Oskoueian, E., Es-Haghi, A., and Yazdi, M. E. T. (2021). Comparative study on the biological effects of sodium citrate-based and apigenin-based synthesized silver nanoparticles. *Nutr. Cancer.* 73, 1511–1519. doi:10.1080/01635581.2020.1801780

Zuorro, A., Iannone, A., Natali, S., and Lavecchia, R. (2019). Green synthesis of silver nanoparticles using bilberry and red currant waste extracts. *Processes* 7, 193–203. doi:10.3390/pr7040193